Vacuum-Ultraviolet absorption and fluorescence spectroscopy of CF_2H_2, CF_2Cl_2 and CF_2Br_2 in the range 8-22 eV

Seccombe, Dominic; Tuckett, Richard; Baumgartel, H; Jochims, HW

DOI:
10.1063/1.1344888

Vacuum–ultraviolet absorption and fluorescence spectroscopy of CF_2H_2, CF_2Cl_2, and CF_2Br_2 in the range 8–22 eV

D. P. Seccombe,[a] R. Y. L. Chim, and R. P. Tuckett[b]
School of Chemistry, University of Birmingham, Edgbaston, Birmingham, B15 2TT, United Kingdom

H. W. Jochims and H. Baumgärtel
Institut fur Physikalische und Theoretische Chemie, Freie Universitat Berlin, Takustrasse 3, D-14195 Berlin, Germany

(Received 8 August 2000; accepted 8 December 2000)

The vacuum–ultraviolet (VUV) absorption and fluorescence spectroscopy of CF_2X_2 (X=H, Cl, Br) in the range 190–690 nm is reported. Tunable vacuum–UV radiation in the range 8–22 eV from synchrotron sources at either Daresbury, U.K. or BESSY1, Germany is used to excite the titled molecules. Fluorescence excitation spectra, with undispersed detection of the fluorescence, were recorded at Daresbury with a resolution of 0.1 nm. VUV absorption spectra at a resolution of 0.08 nm, and dispersed emission spectra with an optical resolution of 8 nm were recorded at BESSY1. Action spectra, in which the VUV energy is scanned with detection of the fluorescence at a specific wavelength, were also recorded at BESSY1 with a resolution of 0.3 nm; appearance energies for production of a particular emitting state of a fragment are then obtained. Using the single-bunch mode of BESSY1, lifetimes of all emitting states that fall in the range ~3–80 ns have been measured. The peaks in the VUV absorption spectra of CF_2X_2 are assigned to Rydberg transitions. For CF_2H_2 below 11 eV, there is good agreement between the absorption and the fluorescence excitation spectra, whereas above 11 eV and for the whole range 8–22 eV for CF_2Cl_2 and CF_2Br_2 there is little similarity. This suggests that photodissociation to emitting states of fragment species represent minor channels. In the range 8–15 eV, emission is due mainly to CF_2 $\tilde{A}\,^1B_1-\tilde{X}\,^1A_1$ and weakly to CFX $\tilde{A}\,^1A''-\tilde{X}\,^1A'$. These products form by photodissociation of Rydberg states of CF_2X_2, and the thresholds for their production, therefore, relate to energies of the Rydberg states of the parent molecule. For CF_2H_2 below 11.18 eV CF_2 $\tilde{A}\,^1B_1$ can only form with H_2, whereas for CF_2Cl_2 and CF_2Br_2 it is not possible to say whether the other products are 2X or X_2. For energies above ~15 eV, emission is due to diatomic fragments; CF $B\,^2\Delta$ and $A\,^2\Sigma^+$, CCl $A\,^2\Delta$, CH $B\,^2\Sigma^-$ and $A\,^2\Delta$, Cl_2 and Br_2 $D'\,2\,^3\Pi_g$, and possibly CBr $A\,^2\Delta$. From their appearance energies, there is evidence that with the exception of CF $B\,^2\Delta/CF_2H_2$ where the ground state of HF must form, the excited state of CF, CCl, or CH forms in association with three atoms. Our results yield no information whether the three bonds in CF_2X_2* break simultaneously or sequentially. We suggest that the anomalous behavior of CF_2H_2, in forming H–H or H–F bonds in unimolecular photofragmentation processes, relates to the small size of the hydrogen atom, and hence, the unimportance of steric effects in the tightly constrained transition state. In no cases is emission observed from excited states of either the CF_2X free radical or the parent molecular ion, $CF_2X_2^+$.
 [DOI: 10.1063/1.1344888]

I. INTRODUCTION

In a previous paper,[1] a comprehensive study of the vacuum–ultraviolet (VUV) fluorescence spectroscopy of CCl_3F, CCl_3H, and CCl_3Br in the range 8–30 eV was presented. VUV photoexcitation of the molecules was followed by the observation of the dispersed fluorescence spectra in the UV/visible. In this paper, we extend this work on halo-substituted methanes to the three CF_2-containing compounds: CF_2H_2, CF_2Cl_2, and CF_2Br_2. Many groups have measured optical emission spectra from these molecules in an attempt to diagnose the emitters produced following VUV excitation. The excitation sources employed have been an ArF laser operating in the multiphoton mode,[2] high-energy electrons,[3–12] fixed-energy gaseous lamps,[13] microwave discharges,[14] and rare-gas metastables.[15] Despite the many advantages of using tunable VUV photons from a synchrotron radiation (SR) source for such studies,[1] only one such study, on CF_2Cl_2, has been reported.[16] For the work presented here, SR from both the Daresbury Laboratory, U.K. and BESSY1, Germany sources is used to perform complimentary fluorescence experiments. These facilities provide continuous radiation in the range 8–30 eV at an operating resolution of 0.1–0.3 nm. Both the VUV excitation energy

[a]Present Address: Physics Department, The University, Newcastle-upon-Tyne, NE1 7RU, U.K.
[b]Author to whom correspondence should be addressed; electronic mail: r.p.tuckett@bham.ac.uk

E_1 and the UV/visible emission wavelength λ_2/ may be defined, providing a flexibility that is usually not available with other sources.

Experiments performed on the CF_3X (X=F, H, Cl, Br) (Ref. 17) and CCl_3X (X=F, H, Br) (Ref. 1) series showed that these two sets of molecules exhibit different behavior following VUV photoexcitation. In CF_3X, emission was observed from the parent ion and the tetra-atomic radical CF_3, whereas no such evidence was found for the analogous emitters in CCl_3X. By contrast, emission was observed from the same valence states of CF_2, CCl_2, CF, and CCl. It is, therefore, of considerable interest to discover what fragments are formed following photoexcitation of the lower-symmetry CF_2X_2 molecules, in particular, CF_2Cl_2. In the CCl_3X study,[1] there were considerable difficulties in assigning transitions observed in the fluorescence excitation spectra. This was due to the low resolution of the spectra, and to the fact that only the Rydberg states of CCl_3X which dissociate to fluorescing fragments were detected. For the CF_2X_2 series of molecules, therefore, in addition to the fluorescence experiments, windowless VUV absorption spectra at an improved resolution of 0.08 nm were recorded at BESSY1. Absorption spectra are considerably easier to assign, and comparison of the two experiments has the potential to reveal quantitative information on the branching ratio to the fluorescing fragments. In some circumstances, information about the dissociation dynamics may also be deduced.

II. EXPERIMENT

Complimentary fluorescence experiments are performed at the synchrotron radiation sources at Daresbury and BESSY1. At Daresbury, the fluorescence chamber, an evacuated stainless-steel cube (side=15 cm), is attached to the storage ring of the synchrotron via a 5 m McPherson normal-incidence monochromator (operating resolution =0.05–0.10 nm). Gas is admitted into the chamber through a hyperdermic needle whose tip is located ~3 mm above the interaction region. Typical operating pressures are 5×10^{-4}–2×10^{-3} Torr compared with a base pressure of 1×10^{-7} Torr. The UV/visible fluorescence resulting from interaction of the VUV photon radiation with the gas molecules is focused by an aluminum-coated spherical concave mirror through a quartz window and detected by a photon-counting photomultiplier tube (PMT), range ~190–650 nm. The range of wavelengths that can be detected may be controlled by an optical filter located between the quartz window and the PMT. The directions of the VUV photon beam, the gas flow, and the fluorescence detection are mutually orthogonal. This experiment enables the measurement of a fluorescence excitation spectrum, the detection of fluorescence intensity as a function of excitation energy. The VUV photon flux is measured via the visible fluorescence from a sodium salicylate window located behind the interaction region. This enables *in situ* flux normalization of the spectra. Data acquisition and scanning of the monochromator are controlled by a dedicated personal computer (PC) interacting with CAMAC electronics.

At BESSY1, the fluorescence chamber, a brass cube of side 5 cm, is attached to the storage ring of the synchrotron via a 1.5 m McPherson normal-incidence monochromator (operating resolution=0.3 nm for fluorescence measurements) and two stages of differential pumping. Sample gas is admitted directly into the fluorescence chamber using a high-precision-needle valve. Typical operating pressures are in the range 5×10^{-3}–1×10^{-2} mbar. The interaction region is located at the center of the brass cube. The resulting fluorescence is dispersed by a 20 cm focal length Jobin Yvon H20VIS visible–ultraviolet monochromator (recipricol dispersion=4 nm mm^{-1}). This ''secondary'' monochromator has a 2 mm exit slit and no entrance slit, yielding an effective spectral resolution of 8 nm. The range of wavelengths that can be detected is ~190–690 nm. The fluorescence is detected by a red-sensitive Hamamtsu R6060 PMT (risetime=1.5 ns) cooled to 280 K. Data acquisition and scanning of the two monochromators are controlled by a dedicated PC interacting with purpose-built electronics. In the multibunch (pseudo-continuous) mode of the synchrotron, three experiments are performed. First, fluorescence excitation spectra are obtained by setting the secondary monochromator to zero order and scanning the energy E_1 of the primary VUV monochromator. Second, E_1 is fixed and the wavelength of emission λ_2 is scanned to yield a dispersed fluorescence spectrum. Third, λ_2 is set to isolate one emission band so, by scanning E_1, an action spectrum is obtained from which an appearance energy associated with a particular excited fragment may be determined. Comparison with thermochemistry may then yield important information regarding the identity of the dominant dissociation channel. Unlike experiments at Daresbury, it is not possible to monitor the VUV photon flux directly during a measurement. Instead, a separate experiment must be performed where a flux curve is measured using the fluorescence from a sodium salicylate window. These data are then employed, retrospectively, to flux normalize the action and fluorescence excitation spectra. No attempt is made to normalize the dispersed fluorescence spectra to the variation in sensitivity of the secondary monochromator with wavelength. The single-bunch mode at BESSY1 can be used to measure fluorescence lifetimes.[1] In this mode where the molecules are excited only every 208 ns, time-resolved fluorescence measurements may be made. The real-time fluorescence decays are analyzed by a nonlinear least-squares-fitting program, FLUORX_ERR,[18] and lifetimes of emitting states are determined. The lifetimes that can be measured are limited to the range ~3–80 ns by the response time of the PMT and the repetition rate of the pulsed excitation source.

VUV absorption spectra were also recorded at BESSY1. The absorption cell is attached to the exit slit of the 1.5 m McPherson normal-incidence monochromator (resolution now improved to 0.08 nm) via two stages of differential pumping. The absorption cell has a path length of 30 cm, and is linked to the final stage of differential pumping by a collimated mesh.[19] Gas is admitted directly into the cell using a high-precision-needle valve. Operating pressures depend on the magnitude of the absorption cross sections being measured, typical values being in the range 20–60 μbar. The VUV flux at the end of the cell is measured by a photon-counting EMI 9789B PMT via the visible fluorescence of a

sodium salicylate window. Since the pressure of the gas and the optical path length are known, measurement of the ratio of transmission functions observed for background (no gas) and sample spectra (with gas) can yield, via the Beer–Lambert law, absolute absorption cross sections. In the calculation of I_0/I at every value of E_1, allowance is made for the (natural) decay of the VUV flux over the time of an experiment. We estimate that our cross sections are accurate to ~15%.

III. ENERGETICS OF THE KEY DISSOCIATION CHANNELS

As the emitters from VUV-excited CF_2X_2 are predicted to be either excited states of the parent ion or neutral fragments produced by photodissociation, thermochemical evaluation of dissociation channels and experimental determination of ionization energies are of considerable importance in analyzing the data. Many groups have measured He I and He II photoelectron spectra.[20–28] Selected values are listed in Table I. The energies of the key dissociation channels of CF_2X_2 (X=H, Cl, Br) are also listed in Table I. The ground-state energies were generally calculated from enthalpies of formation at 0 K given in the JANAF tables.[29] Where values were not available, data at 298 K from Lias *et al.*[30] were used. The enthalpies of formation for CFBr and CF_2Br are not available, hence, energies for the dissociation channels involving these fragments are unknown. The energies of the excited states of most of the emitting fragments were taken from standard sources.[31,32] The energies of the $D'\,^3\Pi_g$ ion-pair state of Cl_2 and Br_2 were taken from Tellinghuisen and co-workers.[33]

IV. RESULTS

A. CF_2H_2

The absorption spectrum of CF_2H_2 was recorded at BESSY1 from 8 to 21 eV at a resolution of 0.08 nm (Fig. 1, upper spectrum). In C_{2v} symmetry, the electronic configuration of the outervalence molecular orbitals of the parent molecule is: $(2a_1)^2(1b_2)^2(3a_1)^2(2b_1)^2(1a_2)^2(4a_1)^2(3b_1)^2(2b_2)^2$,[23] where the numbering scheme does not include core orbitals. Absorption spectra have been measured before,[21,34–36] with absolute values of the cross sections first being determined to an accuracy of ~25% by Edwards and Raymonda for excitation energies below 11.40 eV.[36] Their values are in good agreement to those presented here, even though the resolution employed, 0.2 nm, was significantly inferior. This is somewhat surprising since it is well known that the linewidths of absorption peaks, their peak heights, and hence, the derived cross sections depend on the optical resolution of the VUV photon source.

The assignment of the absorption bands observed in Fig. 1 is now discussed. Below 13 eV, four bands are observed peaking at 9.28, ~10.3, ~11.1 and 12.38 eV (bands I–IV in Fig. 1). In agreement with Brundle, Robin, and Basch,[21] they are assigned to the $2b_2-3s$, $2b_2-3p$, $3b_1-3s$, and $3b_1-3p$ transitions, respectively. Quantum defects of the Rydberg orbitals (Table II) have been determined using the well-known formula

$$E = \mathrm{IE} - \frac{R_H}{(n-\delta)^2}, \tag{1}$$

where E is the energy of the transition, IE is the ionization energy to which the Rydberg state converges, R_H is the Rydberg constant, and n and δ are the principle quantum number and the quantum defect of the Rydberg orbital, respectively. The IEs required were taken from a number of sources, the details being given as footnotes to Table II. For bands with no resolved structure, vertical IEs are used,[20,22] for reasons explained elsewhere.[1] For bands showing vibrational structure, vibrationally resolved IEs with the same vibrational quantum number in the Rydberg state are used.

Bands I and IV are structureless, whereas considerable vibrational structure is resolved in bands II and III. Band II consists of five or six peaks with a constant spacing of $1107\pm50\,\mathrm{cm}^{-1}$. This value is in reasonable agreement with the separation determined by Wagner and Duncan,[34] 1074 cm^{-1}, from their VUV absorption spectrum. A similar result has been obtained for the vibrational structure resolved in the $(2b_2)^{-1}$ ionization band, $1105\pm5\,\mathrm{cm}^{-1}$,[21] and attributed to excitation of the ν_2 (a_1:CH_2 scissors) and ν_3 (a_1:CF_2 stretch) modes. The corresponding vibrational wave numbers in the ground state of the neutral molecule are 1508 and 1116 cm^{-1}.[29] The most recent photoelectron spectrum measured by Pradeep and Shirley showed evidence of three vibrational progressions in the $(2b_2)^{-1}$ band.[23] These were attributed to excitation of the ν_2, ν_3, and $2\nu_4$ (a_1:CF_2 scissors) modes of motion, and the vibrational wave numbers were measured as 1150 ± 5, 1162 ± 5, and $(2\times527)\,\mathrm{cm}^{-1}$, respectively. The identification of the near-degenerate ν_2 and ν_3 progressions was made possible by the high energy resolution employed, ~8 cm^{-1}. The presence of C–F vibrations is hardly surprising since the $2b_2$ orbital is known to have significant fluorine lone-pair character.[21] Indeed, the quantum defects determined from the energies of the valence-Rydberg transitions originating from the $2b_2$ orbital (Table II), are very close to the accepted values for an isolated fluorine atom, 1.20 and 0.75, for s and p orbitals, respectively.[37]

The appearance of vibrational structure in band III ($3b_1\rightarrow3s$) is intriguing since band I ($2b_2\rightarrow3s$) is continuous and unstructured. These observations imply that dissociation of the $(3b_1)^{-1}3s$ Rydberg state is slower than that of the $(2b_2)^{-1}3s$ state. These states have term symbols $^2B_1$ and $^2B_2$, respectively. The difference in symmetry of these two Rydberg states may cause one to dissociate slower than the other. The first six members of the progression in band III have a constant separation of $400\pm60\,\mathrm{cm}^{-1}$; the splitting of the higher members becomes greater. Two groups have suggested that excitation in at least two modes (ν_3 and ν_4) is responsible for the observed vibrational structure.[21,34] Pradeep and Shirley,[23] however, have found insufficient evidence of this in their high-resolution photoelectron spectrum of the $\tilde{A}\,^2B_1$ band. They determine a vibrational frequency of 583 cm^{-1} and attribute it to the ν_4 mode. Unfortunately, the vibrationally resolved ionization energies were not reported,

TABLE I. Energetics of the key dissociation channels and ionization energies of CF_2H_2, CF_2Cl_2, and CF_2Br_2.

Molecule	Ion	Dissociation channel	Adiabatic (vertical) IE/eV	Dissociation energy/eV
CF_2H_2		$CH+H^*(n=6)+2F$		27.78
		$CH+H^*(n=6)+F_2$		26.18
		$CF+F+H+H^*(n=6)$		25.71
		$CFH+F+H^*(n=6)$		22.16
		$CF_2+H^*(n=6)+H$		20.41
		$CF+HF+H^*(n=6)$		19.85
		$CF\ B\ ^2\Delta+2H+F$		18.60
	$CF_2H_2^+\ \tilde{F}\ ^2B_2$		18.270[a] (18.97,[b] 19.13[c])	
	$CF_2H_2^+\ \tilde{E}\ ^2A_1$		18.236[a] (18.97,[b] 19.13[c])	
	$CF_2H_2^+\ \tilde{D}\ ^2B_1$		18.208[a] (18.97,[b] 19.13[c])	
		$CH\ B\ ^2\Sigma^-+H+2F$		17.78
		$CF\ A\ ^2\Sigma^++2H+F$		17.77
		$CF_2H+H^*(n=6)$		17.60
		$CH\ A\ ^2\Delta+H+2F$		17.42
		$CH\ B\ ^2\Sigma^-+F_2+H$		16.18
		$CH\ A\ ^2\Delta+H+F_2$		15.82
	$CF_2H_2^+\ \tilde{C}\ ^2A_2$		15.624[a] (15.58,[b] 15.71[c])	
	$CF_2H_2^+\ \tilde{B}\ ^2A_1$		15.572[a] (15.58,[b] 15.71[c])	
	$CF_2H_2^+\ \tilde{A}\ ^2B_1$		14.611[a] (15.25[b])	
		$CF\ B\ ^2\Delta+H_2+F$		14.12
		$CF\ A\ ^2\Sigma^++H_2+F$		13.29
		$CF\ B\ ^2\Delta+HF+H$		12.74
	$CF_2H_2^+\ \tilde{X}\ ^2B_2$		12.729[a] (13.29[b])	
		$CH\ B\ ^2\Sigma^-+HF+F$		11.92
		$CF\ A\ ^2\Sigma^++HF+H$		11.91
		$CF_2\ \tilde{A}\ ^1B_1+2H$		11.80
		$CH\ A\ ^2\Delta+HF+F$		11.56
		$CH_2\ \tilde{b}\ ^1B_1+2F$		11.46
		$CFH\ \tilde{A}\ ^1A''+F+H$		11.07
		$CH_2\ \tilde{b}\ ^1B_1+F_2$		9.86
		$CF_2\ \tilde{A}\ ^1B_1+H_2$		7.32
		$CFH\ \tilde{A}\ ^1A''+FH$		5.21
CF_2Cl_2	$CF_2Cl_2^+\ \tilde{K}\ ^2A_1$		(22.4[d])	
		$Cl_2\ D'\ 2\ ^3\Pi_g+C+2F$		21.13
	$CF_2Cl_2^+\ \tilde{J}\ ^2B_2$		(20.4[d])	
		$Cl_2\ D'\ 2\ ^3\Pi_g+C+F_2$		19.53
	$CF_2Cl_2^+\ \tilde{H}\ ^2A_1/\tilde{I}\ ^2B_1$		(19.3[d])	
		$CCl\ A\ ^2\Delta+2F+Cl$		17.50
		$CF\ B\ ^2\Delta+F+2Cl$		17.06
	$CF_2Cl_2^+\ \tilde{G}\ ^2A_1$		(16.90[d])	
	$CF_2Cl_2^+\ \tilde{F}\ ^2A_2$		(16.30[d])	
		$CF\ A\ ^2\Sigma^++F+2Cl$		16.23
		$CCl\ A\ ^2\Delta+F_2+Cl$		15.90
	$CF_2Cl_2^+\ \tilde{E}\ ^2B_1$		(15.90[d])	
		$Cl_2\ D'\ 2\ ^3\Pi_g+CF+F$		15.56
		$CCl\ A\ ^2\Delta+FCl+F$		14.94
		$CF\ B\ ^2\Delta+F+Cl_2$		14.58
		$CF\ B\ ^2\Delta+FCl+Cl$		14.50
	$CF_2Cl_2^+\ \tilde{D}\ ^2B_2$		14.126[a] (14.36[d])	
		$CF\ A\ ^2\Sigma^++F+Cl_2$		13.75
		$CF\ A\ ^2\Sigma^+FCl+Cl$		13.67
	$CF_2Cl_2^+\ \tilde{C}\ ^2A_1$		(13.45[d])	
	$CF_2Cl_2^+\ \tilde{B}\ ^2A_2$		13.078[a] (13.11[d])	
	$CF_2Cl_2^+\ \tilde{A}\ ^2B_1$		(12.53[d])	
	$CF_2Cl_2^+\ \tilde{X}\ ^2B_2$		11.734[a] (12.26[d])	
		$CCl_2\ \tilde{A}\ ^1B_1+2F$		11.25
		$Cl_2\ D'\ 2\ ^3\Pi_g+CF_2$		10.26
		$CF_2\ \tilde{A}\ ^1B_1+2Cl$		10.26
		$CClF\ \tilde{A}\ ^1A''+Cl+F$		10.01
		$CCl_2\ \tilde{A}\ ^1B_1+F_2$		9.65
		$CF_2\ \tilde{A}\ ^1B_1+Cl_2$		7.78
		$CClF\ \tilde{A}\ ^1A''+FCl$		7.45

TABLE I. (*Continued.*)

Molecule	Ion	Dissociation channel	Adiabatic (vertical) IE/eV	Dissociation energy/eV
CF_2Br_2	$CF_2Br_2^+ \tilde{K}\,^2A_1$		(22.5[e])	
	$CF_2Br_2^+ \tilde{J}\,^2B_2$		(20.0[e])	
	$CF_2Br_2^+ \tilde{I}\,^2A_1$		(19.0[e])	
		$Br_2\,D'\,2\,^3\Pi_g + C + 2F$		18.97
	$CF_2Br_2^+ \tilde{H}\,^2B_1$		(18.69[e])	
		$Br_2\,D'\,2\,^3\Pi_g + C + F_2$		17.37
	$CF_2Br_2^+ \tilde{G}\,^2A_1$		(16.37[e])	
		$CBr\,A\,^2\Delta + 2F + Br$		16.13
		$CF\,B\,^2\Delta + 2Br + F$		15.90
	$CF_2Br_2^+ \tilde{E}\,^2A_2/\tilde{F}\,^2B_1$		(15.57[e])	
		$CF\,A\,^2\Sigma^+ + 2Br + F$		15.07
		$CBr\,A\,^2\Delta + F_2 + Br$		14.53
		$CBr\,A\,^2\Delta + FBr + F$		13.58
		$CF\,B\,^2\Delta + Br_2 + F$		13.46
		$Br_2\,D'\,2\,^3\Pi_g + CF + F$		13.41
		$CF\,B\,^2\Delta + BrF + Br$		13.35
	$CF_2Br_2^+ \tilde{D}\,^2B_2$		(13.22[e])	
		$CF\,A\,^2\Sigma^+ + Br_2 + F$		12.63
		$CF\,A\,^2\Sigma^+ + BrF + Br$		12.52
	$CF_2Br_2^+ \tilde{C}\,^2A_1$		(12.41[e])	
	$CF_2Br_2^+ \tilde{B}\,^2A_2$		(12.06[e])	
	$CF_2Br_2^+ \tilde{A}\,^2B_1$		(11.56[e])	
	$CF_2Br_2^+ \tilde{X}\,^2B_2$		(11.17[e])	
		$CF_2\tilde{A}\,^1B_1 + 2Br$		9.10
		$Br_2\,D'\,2\,^3\Pi_g + CF_2$		8.11
		$CF_2\tilde{A}\,^1B_1 + Br_2$		6.66

[a]Reference 23.
[b]Reference 20.
[c]Reference 22.
[d]Reference 24.
[e]Reference 27.

only the adiabatic ionization energy for the overall band. It was, therefore, not possible to assign unambiguously the vibrational peaks in the absorption band. The quantum defect associated with the lowest-energy transition is given in Table II. Its value, 1.08, is characteristic of an isolated fluorine *s* orbital, 1.20.[37]

The region of the spectrum above 13 eV has never been assigned. Between 13 and 20 eV, four structureless features

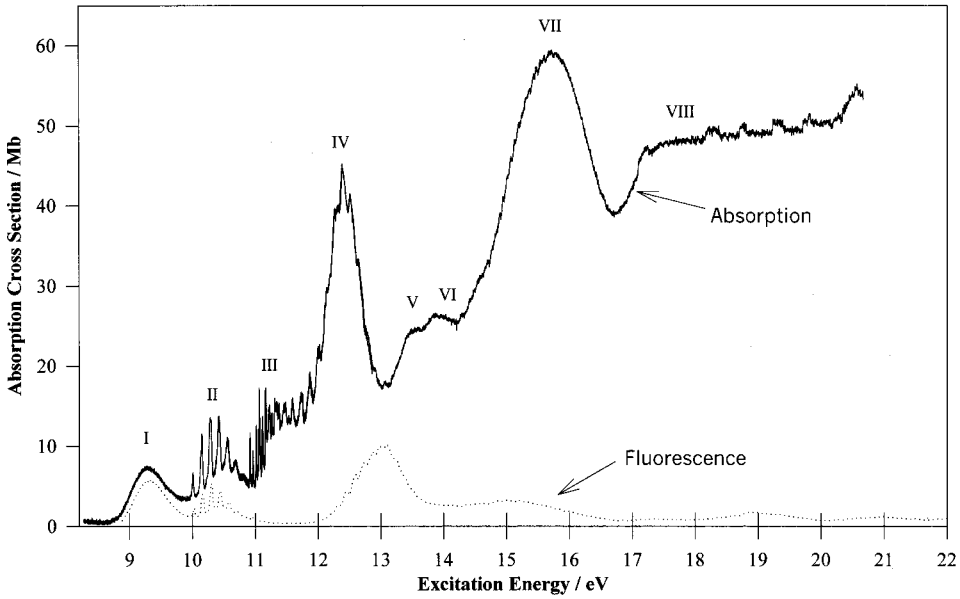

FIG. 1. Vacuum–UV absorption (upper spectrum) and fluorescence excitation (lower spectrum) spectra of CF_2H_2 recorded at the BESSY1 synchrotron source. The resolution of the spectra are 0.08 and 0.3 nm, respectively. Absorption cross sections are measured in units of Mb (1 Mb $=10^{-18}$ cm^2), fluorescence cross sections in arbitrary units.

TABLE II. Assignment of the vacuum–UV absorption bands in CF_2H_2.

Band	Peak position/eV	Assignment	IE/eV	δ
I	9.28	$2b_2-3s$	13.29[a]	1.16
II	10.01	$2b_2-3p(0,0)$	12.729[b]	0.76
	10.15	$2b_2-3p(0,1)$	12.872[b]	0.76
	10.29	$2b_2-3p(0,2)$	13.010[b]	0.77
	10.42	$2b_2-3p(0,3)$	13.195[b]	0.79
	10.55	$2b_2-3p(0,4)$	13.278[b]	0.77
	10.69	$2b_2-3p(0,5)$	13.407[b]	0.76
III	10.91	$3b_1-3s(0,0)$	14.611[b]	1.08
IV	12.38	$3b_1-3p$	15.25[a]	0.82
V	13.56	$4a_1-3s$ or $1a_2-3s$	15.71[c]	0.48
VI	13.86	$4a_1-3p$ or $1a_2-3p$	15.71[c]	0.29
VII	15.72	$1b_2-3s$ or $3a_1-3s$ or $2b_1-3s$	19.13[c]	1.00

[a]Reference 20.
[b]Reference 23.
[c]Reference 22.

are observed, and the spectrum is undoubtedly complicated by the onset of ionization. Using vertical ionization energies and assuming that because of the high electronegativity of the fluorine atom, the quantum defects of the molecular orbitals will, in general, have values similar to those calculated for an isolated fluorine atom, bands V–VII have been tentatively assigned (Table II). The quantum defects determined for bands V and VI are anomalously low, indicating that the Rydberg electron may occupy an orbital which is located predominantly on the carbon and/or hydrogen atoms. Band VIII at ~19 eV has not been assigned. It is extremely broad and probably represents a superposition of many transitions.

The fluorescence excitation spectrum of CF_2H_2 was recorded both at BESSY1 over the range 8–22 eV at a resolution 0.3 nm (Fig. 1, lower spectrum), and at Daresbury over a comparable range at an improved resolution of 0.1 nm (Fig. 2). In Fig. 1, the fluorescence excitation spectrum is presented on an arbitrary ordinate scale, hence, the absolute fluorescence quantum yield cannot be inferred. Below 11 eV, Fig. 1 shows that the fluorescence excitation spectrum resembles the absorption spectrum quite closely, except that the ratio of the intensities of bands I and II is inverted. Above 11 eV, there is little similarity between the spectra. In particular, band III is completely absent in the fluorescence spectrum and the peak of band IV is shifted to higher energy, 13.0 eV. For $E_1 > 13$ eV, it becomes hard to determine the relationship between the absorption and fluorescence bands. Over the whole of the fluorescence excitation spectrum, all the peaks have shapes characteristic of a resonant primary excitation process (i.e., $A + h\nu \rightarrow A^*$, where A^* is a discrete excited state of the parent molecule). This indicates that fluorescence is due to fragment species produced by photodissociation of A^*, or just possibly to A^* itself. Fluorescence from excited states of the parent ion is characterized by a nonresonant primary excitation process [i.e., $A + h\nu \rightarrow (A^+)^* + e^-$], since the photoelectron can carry off the excess energy. The shape of the peak in the fluorescence excitation spectrum is then very different.[17] We note, therefore, that fluorescence from excited states of $CF_2H_2^+$, if present, is exceptionally weak.

Dispersed emission spectra over the range 190–690 nm were recorded at BESSY1 for chosen excitation energies between 9 and 22 eV, corresponding to the peaks in Figs. 1 and 2. The dispersed emission spectrum recorded at $E_1 = 9.29$ eV is shown in Fig. 3(a). As there is a significant amount of second-order radiation from the secondary monochromator for $\lambda_2 > 450$ nm, only the limited range of 190–450 nm is displayed. One broad featureless band stretching from 240 to 370 nm and peaking at 290 nm is observed. The

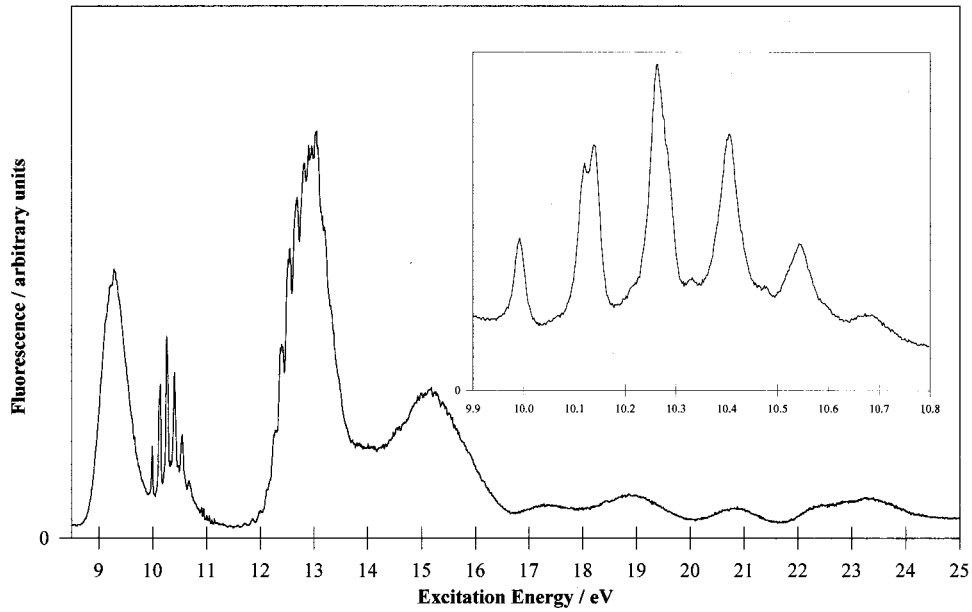

FIG. 2. Vacuum–UV fluorescence excitation spectrum of CF_2H_2 recorded at the Daresbury synchrotron source with a resolution of 0.1 nm. The insert between 9.9 and 10.8 eV was recorded at a resolution of 0.05 nm.

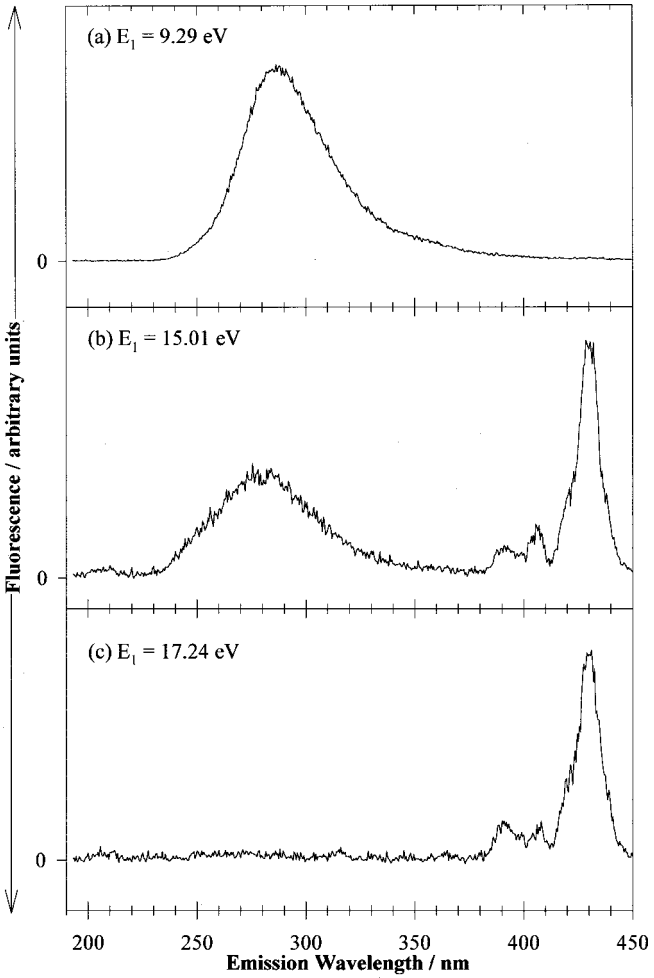

FIG. 3. Dispersed fluorescence spectra recorded at a resolution of 8 nm for CF_2H_2 photoexcited at (a) 9.29 eV, (b) 15.01 eV, and (c) 17.24 eV.

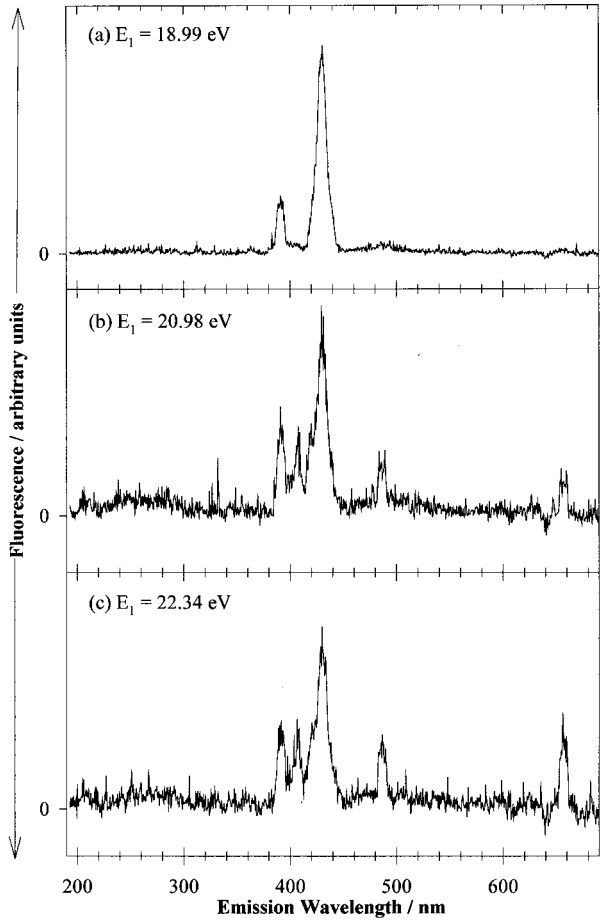

FIG. 4. Dispersed fluorescence spectra recorded at a resolution of 8 nm for CF_2H_2 photoexcited at (a) 18.99 eV, (b) 20.98 eV, and (c) 22.34 eV.

emission is due to the CF_2 $\tilde{A}\,^1B_1-\tilde{X}\,^1A_1$ transition.[38–40] Dispersed spectra were also recorded at the higher excitation energies of 15.01 [Fig. 3(b)], 17.24 [Fig. 3(c)], 18.99 [Fig. 4(a)], 20.98 [Fig. 4(b)], and 22.34 eV [Fig. 4(c)]. Two bands are present in all these five spectra, peaking at 426 and 388 nm. They are assigned to CH $A\,^2\Delta-X\,^2\Pi$ and CH $B\,^2\Sigma^- - X\,^2\Pi$, respectively.[31] For $E_1=15.01$ and 17.24 eV, a band at ~410 nm is present and is probably due to CF $B\,^2\Delta-X\,^2\Pi$ in second order.[31] For $E_1=20.98$ and 22.34 eV there are additional features at 408, 488, and 655 nm. As their appearance energy is quite high and their width considerably narrower than the other bands, it seems likely that these emissions are due to an atomic fragment. The wavelengths are very close to the fourth ($n=6\rightarrow2$), second ($n=4\rightarrow2$), and first lines ($n=3\rightarrow2$) of the Balmer series in atomic hydrogen. The third line ($n=5\rightarrow2$) of this series occurs at 433 nm and is not observed as it lies too close in energy to the intense CH $A-X$ emission. Perhaps the most interesting feature of the dispersed emission spectra is that they seem to indicate that the branching to CH* is much higher than to CF*. This is despite the fact that the thermochemical energies of analogous channels to CH* and CF* are not dissimilar. This effect is probably the result of state-specific dissociation of CH_2H_2*.

Action spectra were recorded at a resolution of 0.3 nm for λ_2 values of 207, 283, and 428 nm, isolating the CF $B-X$, CF_2 $\tilde{A}-\tilde{X}$, and CH $A-X$ emissions, respectively [Figs. 5(a)–5(c)]. Unfortunately, the other emitters could not be isolated, either due to second-order radiation from the secondary monochromator or to overlapping CF_2 $\tilde{A}-\tilde{X}$ emission. Instead, a fluorescence excitation spectrum was recorded at Daresbury with an Oriel 500 cut-on filter. This filter allowed only radiation with $\lambda_2>500$ nm to be detected [Fig. 5(d)]. The spectrum peaks at 15 eV, considerably below the appearance energy for the atomic fragment emission at 655 nm. Hence, another red–visible emitter must be present which was not detected in the dispersed emission spectra because of the large amount of CF_2 $\tilde{A}-\tilde{X}$ in second order. It is likely that this is the CFH $\tilde{A}\,^1A''$ state, and several groups have observed the CFH $\tilde{A}\,^1A''-\tilde{X}\,^1A'$ transition between 430 and 635 nm.[41,42] Appearance energies were measured from the action spectra, and a summary of the emission bands and appearance energies for the emitting fragments is given in Table III. We note the absence of emission in CH_2, CF_2H, and CFH_2.

B. CF_2Cl_2

The absorption spectrum of CF_2Cl_2 was recorded at BESSY1 from 8 to 22 eV at a resolution of 0.08 nm

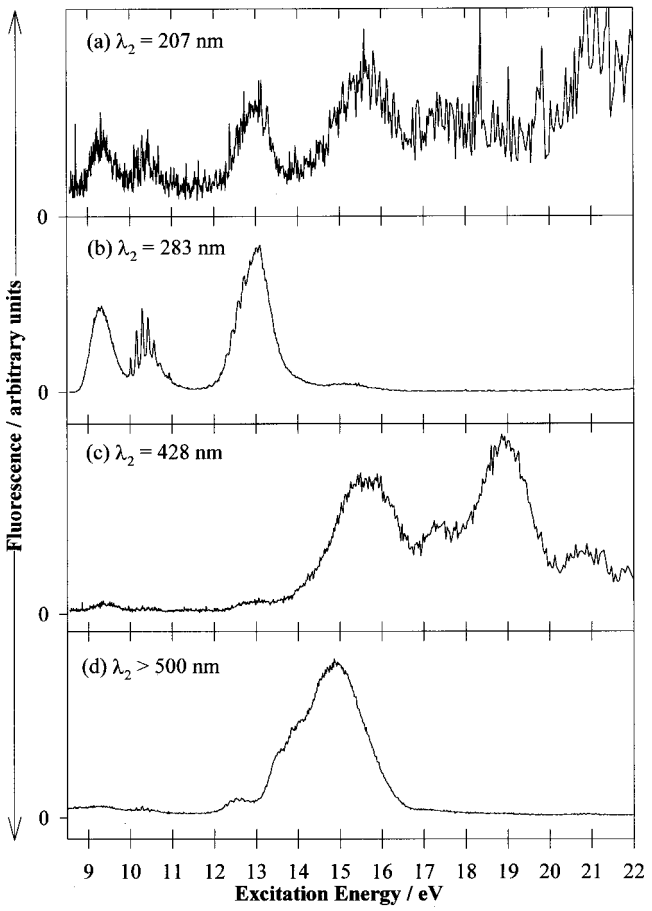

FIG. 5. (a)–(c) Action spectra of CF_2H_2 recorded at the BESSY 1 synchrotron source with a resolution of 0.3 nm for $\lambda_2=207$, 283, and 428 nm, respectively. (d) Fluorescence excitation spectrum of CF_2H_2 recorded at the Daresbury source with a resolution of 0.1 nm. An Oriel 500 filter ensured that only radiation with $\lambda_2>500$ nm was detected.

(Fig. 6 upper spectrum). Absorption cross sections have been determined by a number of groups,[13,35,43–47] and the values shown in Fig. 6 are in good agreement with previous measurements. The electronic configuration of the outervalence molecular orbitals of the molecule is $(3a_1)^2(3a_2)^2(3b_1)^2(3b_2)^2(4a_1)^2(4a_2)^2(4b_1)^2(4b_2)^2$,[13]

TABLE III. Summary of the emission bands identified following VUV photoexcitation of CF_2H_2.

Fragment	Appearance energy/eV	E_1 range/eV	λ_2 range/eV	Assignment
$CF_2\tilde{A}\,^1B_1$	8.7±0.1	8.7–15.8	240–400	$\tilde{A}\,^1B_1-\tilde{X}\,^1A_1$
CFH $\tilde{A}\,^1A''$	12.1±0.1	12.1–16.5	~500	$\tilde{A}\,^1A''-\tilde{X}\,^1A'$
CF $B\,^2\Delta$	12.5±0.3	>12.5	~210	$B\,^2\Delta-X\,^2\Pi$
CH $A\,^2\Delta$	13.8±0.2	>13.8	418–440	$A\,^2\Delta-X\,^2\Pi$
CH $B\,^2\Sigma$	···	···	385–395	$B\,^2\Sigma-X\,^2\Pi$
H($n=3$)[a]	19–21	>19–21	655	$n=3\rightarrow2$
H($n=4$)[a]	19–21	>19–21	488	$n=4\rightarrow2$
H($n=6$)[a]	19–21	>19–21	408	$n=6\rightarrow2$

[a]n is the principle quantum number.

where the numbering scheme does not include core orbitals. The absorption spectrum of CF_2Cl_2 has less-resolved vibrational structure than that of CF_2H_2 recorded at the same resolution of 0.08 nm. Vibrational structure is only observed in band VIII (Fig. 7) with adjacent peaks separated by 225 $\pm70\,cm^{-1}$. It is likely that this corresponds to excitation in the v_4 (CCl_2 scissors: a_1 symmetry) mode whose vibrational frequency in the ground electronic state of CF_2Cl_2 is 261.5 cm^{-1}.[29] The features in the absorption spectrum have been assigned (Table IV), using vertical ionization energies taken from Cvitas, Gusten, and Klansic.[24] The quantum defects obtained are generally in good agreement with those determined for either isolated chlorine ($ns=2.01$, $np=1.57$, $nd=0.09$) or fluorine atoms ($ns=1.20$, $np=0.75$, $nd=0.003$).[37] Care has been taken to ensure that the quantum defect determined for a particular orbital reflects the character of that orbital.

The fluorescence excitation spectrum of CF_2Cl_2 was recorded both at BESSY1 over the range 9–22 eV at a resolution of 0.3 nm (Fig. 6, lower spectrum), and at Daresbury over a comparable range at an improved resolution of 0.1 nm. The spectra are very similar. As with CF_2H_2, the fluorescence excitation spectrum in Fig. 6 is presented on an arbitrary ordinate scale. All peaks have shapes characteristic of a resonant primary excitation process, with fluorescence being due to different fragments of CF_2Cl_2 produced by (pre)dissociation. In contrast to CF_2H_2, below 11.5 eV the absorption and fluorescence spectra show considerable differences. For example, the threshold energy for absorption is 8.7 eV compared to 10.3 eV for fluorescence. Above 11.5 eV, most of the observed absorption bands are present in the fluorescence spectrum, whereas peaks I–IV in the absorption spectra have no corresponding peaks in the fluorescence excitation spectra.

Dispersed fluorescence spectra over the range 190–690 nm were measured at BESSY1 for several excitation energies between 11.3 and 15.5 eV. Spectra for $E_1=11.37$ and 13.04 eV are shown in Figs. 8(a) and 8(b). Due to the problem of second-order radiation from the secondary monochromator, only the limited range of 190–450 nm is displayed. The broad and unstructured CF_2 $\tilde{A}\,^1B_1-\tilde{X}\,^1A_1$ band, stretching from 240 to 370 nm and peaking at 290 nm, dominates both spectra.[38–40] For $E_1=11.37$ eV there is an additional weak shoulder peaking at ~400 nm. It is likely that this is the CFCl $\tilde{A}\,^1A''-\tilde{X}\,^1A'$ transition,[32,48] and it is clear that the relative intensity of the CFCl to CF_2 emission bands decreases as the photon energy increases above 11.37 eV. For excitation energies above 19 eV, the emission spectra are dramatically different [Fig. 8(c)]. Four narrower bands are clearly resolved at 207, 255, 278, and 305 nm. These are assigned to CF $B\,^2\Delta-X\,^2\Pi$, Cl_2 $D'2\,^3\Pi_g-A'2\,^3\Pi_u$, CCl $A\,^2\Delta-X\,^2\Pi$, and an unassigned band in Cl_2, respectively. Some of the emission in the 255 nm band may also be due to CF $A\,^2\Sigma^+-X\,^2\Pi$. In our earlier work on CF_2Cl_2 at Daresbury,[16] where filters were the only means to determine the wavelength range of the emissions, we believed that emission induced at $\sim E_1=20$ eV to be predominantly due to the CF $A\,^2\Sigma^+$ state. This is clearly wrong, and shows the importance of the dispersed fluorescence experiment we

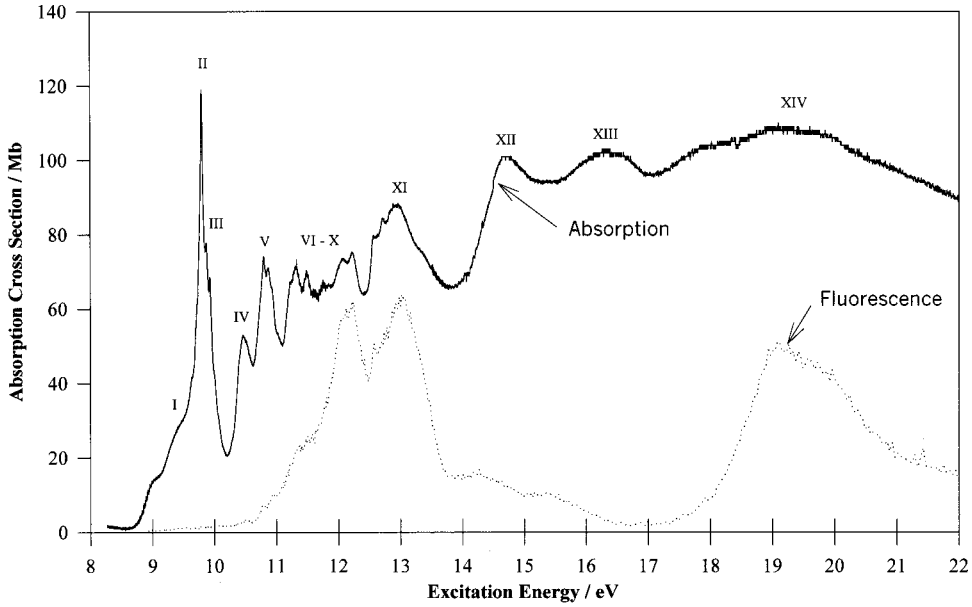

FIG. 6. Vacuum–UV absorption (upper spectrum) and fluorescence excitation (lower spectrum) spectra of CF_2Cl_2 recorded at the BESSY 1 synchrotron source. The resolution of the spectra are 0.08 and 0.3 nm, respectively. Absorption cross sections are measured in units of Mb ($1\,\text{Mb} = 10^{-18}\,\text{cm}^2$), fluorescence cross sections in arbitrary units.

have developed at the BESSY1 source. Unlike CF_2H_2, no atomic emission lines are observed from CF_2Cl_2 for VUV excitation energies around 20 eV.

Action spectra were recorded at BESSY1 with a resolution of 0.3 nm. They could only unambiguously be recorded for $\lambda_2 = 207$ and 300 nm, isolating the CF $B-X$ and CF_2 $\tilde{A}-\tilde{X}$ bands, respectively [Figs. 9(a) and 9(b)]. We note that the action spectrum for formation of CF $B\,^2\Delta$ from CF_2Cl_2 is very different in form to that from CF_2H_2 [Fig. 5(a)]. In addition, fluorescence excitation spectra were recorded at Daresbury with Schott GG395 and Oriel 500 cut-on filters [Figs. 9(c) and 9(d)], constituting pseudo-action spectra with $\lambda_2 > 395$ and $\lambda_2 > 500\,\text{nm}$, respectively. Since the intensity of CF_2 $\tilde{A}-\tilde{X}$ emission is extremely low at wavelengths above 400 nm, other higher-wavelength emitters must be responsible for the signal observed in Figs. 9(c) and 9(d). As the two spectra are considerably different, more than one, as yet unassigned, emitter must be present at wavelengths above 400 nm. In all probability the emissions are caused by CCIF $\tilde{A}-\tilde{X}$ and CCl_2 $\tilde{A}\,^1B_1-\tilde{X}\,^1A_1$ transitions with electronic origins at 396 and 580 nm, respectively.[32] It is likely that the GG395 filter transmits both CFCl and CCl_2 $\tilde{A}-\tilde{X}$ emission, while the Oriel 500 filter transmits predominantly CCl_2 $\tilde{A}-\tilde{X}$ emission. We presume that CCl_2 emission was not detected in the dispersed emission spectra because of the large intensity of CF_2 $\tilde{A}-\tilde{X}$ in second order. Appearance energies have been determined from the action spectra, and a summary of the emission bands for VUV-excited CF_2Cl_2 is given in Table V.

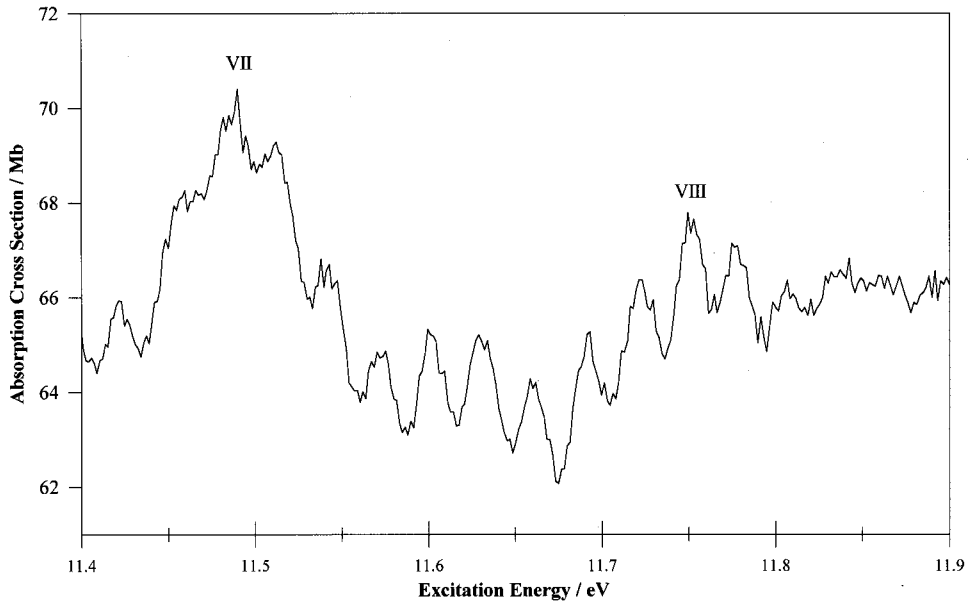

FIG. 7. Vacuum–UV absorption spectrum of CF_2Cl_2 over the range 11.4–11.9 eV.

TABLE IV. Assignment of the absorption bands in CF_2Cl_2.

Band	Peak position/eV	Assignment	IE/eV[a]	δ
I	9.63	$4a_2-4s$	13.11	2.02
II	9.79	$4b_2-4p$	12.26	1.57
III	10.0	$4a_1-4s$	13.45	2.01
IV	10.46	$4b_1-4p$	12.53	1.87
		or $4b_2-3d$	12.26	0.25
V	10.84	$4a_2-4p$	13.11	1.55
VI	11.33	$4a_1-4p$	13.45	1.47
		or $3b_2-4s$	14.36	1.88
VII	11.49	$4a_2-3d$	13.11	0.10
VIII	11.75	$4a_1-3d$	13.45	0.17
		or $3b_1-3s$	15.90	1.19
IX	12.07	$3b_2-4p$	14.36	1.56
X	12.22	$3b_2-4p$	14.36	1.48
XI	12.96	$3b_2-5s$	14.36	1.88
XII	14.72	$3b_1-4p$	15.90	0.60
		or $3a_2-4s$	16.30	1.07
		or $3a_1-4p$	16.90	1.50
XIII	~16.5	$2b_1-nl$	19.3	···
		or $2a_1-nl$	19.3	···

[a]Vertical ionization energies from Ref. 24.

C. CF_2Br_2

The absorption spectrum of CF_2Br_2 was recorded at BESSY1 from 7 to 22 eV at a resolution of 0.08 nm (Fig. 10, upper spectrum). No vibrational structure is observed at this resolution. Absorption cross sections have been measured previously by Doucet *et al.*,[26] and the two sets of values are in reasonable agreement. The electronic configuration of the outervalence orbitals of this molecule is $(3a_1)^2(3a_2)^2(3b_1)^2(3b_2)^2(4a_1)^2(4a_2)^2(4b_1)^2(4b_2)^2$,[27] where the numbering scheme does not include core orbitals. Cvitas *et al.*[27] measured ionization energies by He I photoelectron spectroscopy which were used to assign the Rydberg transitions observed in the absorption spectrum (Table VI). In contrast to CCl_3Br,[49] no spin-orbit splitting was observed in the He I spectrum since all the states of the parent ion of CF_2Br_2 are orbitally singly degenerate. The highest-lying molecular orbitals of CF_2Br_2 are dominated by bromine lone-pair character, so that the lower-energy transitions in the absorption spectrum have associated quantum defects which are close to the values calculated for an isolated bromine atom ($ns=2.96$, $np=2.51$, $nd=1.10$) (see Table VI).[37]

The fluorescence excitation spectrum of CF_2Br_2 was recorded both at BESSY1 over the range 9–22 eV at a resolution of 0.3 nm (Fig. 10, lower spectrum), and at Daresbury at a resolution of 0.1 nm. The spectra were very similar. As with CF_2H_2 and CF_2Cl_2, the fluorescence excitation spectrum in Fig. 10 is presented on an arbitrary ordinate scale, and all the peaks have a shape which is characteristic of a resonant primary excitation process. The threshold energy of the fluorescence spectrum, 9.2 eV, is considerably higher than that for absorption, 7.4 eV, behavior mirroring that of CF_2Cl_2. Furthermore, the spectra bear little resemblance to each other below 11 eV. At higher energies, especially between 11 and 12.5 eV, many of the observed absorption features can be found in the fluorescence spectrum.

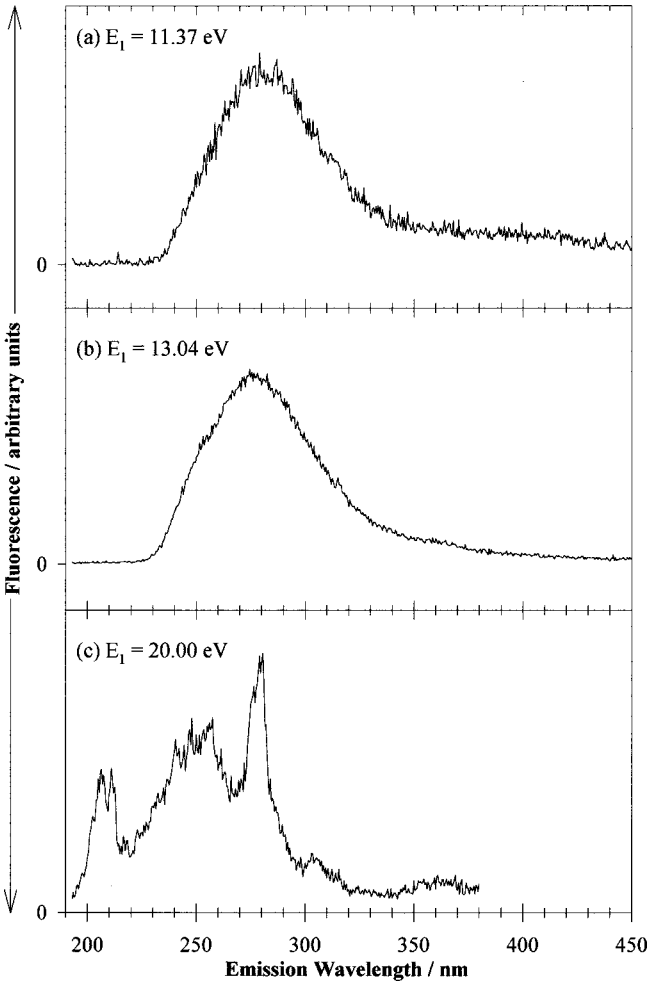

FIG. 8. Dispersed fluorescence spectra recorded at a resolution of 8 nm for CF_2Cl_2 photoexcited at (a) 11.37 eV, (b) 13.04 eV, and (c) 20.00 eV.

Dispersed emission spectra over the range 190–690 nm were measured for $E_1=9.76$, 11.09, 13.30, 15.30, 17.87, and 22.63 eV (Figs. 11 and 12). As before, only the low-wavelength section is displayed because of second-order radiation from the secondary monochromator. For E_1 in the range 9–13 eV, the spectra are dominated by the broad CF_2 $\tilde{A}-\tilde{X}$ emission. For $E_1=13.30$ eV two additional narrow bands are present at 290 and 353 nm. These are attributed to transitions in Br_2,[31] the former being the $D'2\,^3\Pi_g-A'2\,^3\Pi_u$ ion pair to valence transition. At the higher excitation energies the CF_2 $\tilde{A}-\tilde{X}$ band disappears, while the Br_2 bands remain. For $E_1=22.63$ eV, only the band at 290 nm is present to a significant degree.

Action spectra between 9 and 22 eV were measured at BESSY1 with a resolution of 0.3 nm for $\lambda_2=207$ and 313 nm, isolating the CF $B\,^2\Delta-X\,^2\Pi$ and CF_2 $\tilde{A}\,^1B_1-\tilde{X}\,^1A_1$ bands, respectively [Figs. 13(a) and 13(b)]. As with CF_2Cl_2, fluorescence excitation spectra were recorded, in addition, at Daresbury using Schott GG395 and Oriel 500 cut-on filters

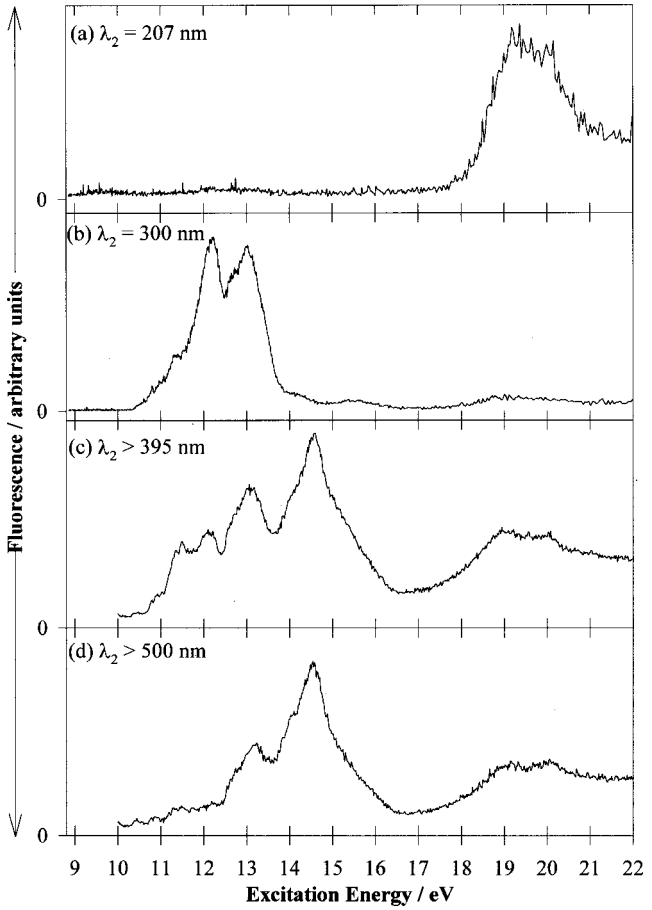

FIG. 9. (a)–(b) Action spectra of CF_2Cl_2 recorded at the BESSY1 synchrotron source with a resolution of 0.3 nm for $\lambda_2=207$ and 300 nm, respectively. (c)–(d) Fluorescence excitation spectra of CF_2Cl_2 recorded at the Daresbury source with a resolution of 0.1 nm. Optical filters ensured that only radiation with (c) $\lambda_2>395$ nm and (d) $\lambda_2>500$ nm was detected.

[Figs. 13(c) and 13(d)]. The fluorescence observed at $\lambda_2>400$ nm in Figs. 13(c) and 13(d) is in all probability due to CBr_2 $\tilde{A}\,^1B_1-\tilde{X}\,^1A_1$ or CFBr $\tilde{A}\,^1A''-\tilde{X}\,^1A'$, which are known to occur at 560–660 and 420–470 nm, respectively.[50,51] It is likely that both these emitters are present since the GG395 and Oriel 500 spectra are different. In all probability, the GG395 filter transmits fluorescence from both CFBr and CBr_2 $\tilde{A}-\tilde{X}$, while the Oriel 500 filter transmits only CBr_2 $\tilde{A}-\tilde{X}$ emission. Appearance energies have been determined from the action spectra, and a summary of the emission bands from VUV-excited CF_2Br_2 is given in Table VII.

TABLE V. Summary of the emission bands identified following VUV photoexcitation of CF_2Cl_2.

Fragment	Appearance energy/eV	E_1 range/eV	λ_2 range/nm	Assignment
CF_2 $\tilde{A}\,^1B_1$	10.4 ± 0.1	10.4–15.0	230–400	$\tilde{A}\,^1B_1-\tilde{X}\,^1A_1$
CFCl $\tilde{A}\,^1A''$	⋯	⋯	~400	$\tilde{A}\,^1A''-\tilde{X}\,^1A'$
CCl_2 $\tilde{A}\,^1B_1$	⋯	⋯	~500	$\tilde{A}\,^1B_1-\tilde{X}\,^1A_1$
Cl_2 $D'\,2\,^3\Pi_g$	>15.5	>15.5	~255	$D'\,2\,^3\Pi_g-A'\,2\,^3\Pi_u$
Cl_2^*	>15.5	>15.5	~305	$D'\,2\,^3\Pi_g-?$
CF $A\,^2\Sigma^+$	>15.5	>15.5	~230	$A\,^2\Sigma^+-X\,^2\Pi$
CF $B\,^2\Delta$	18.1 ± 0.2	>18.1	200–215	$B\,^2\Delta-X\,^2\Pi$
CCl $A\,^2\Delta$	>15.5	>15.5	260–280	$A\,^2\Delta-X\,^2\Pi$

D. Lifetime measurements

Using the single-bunch mode of BESSY1, the lifetimes of the emitting states which fall in the range ~3–80 ns produced by VUV photoexcitation of CF_2X_2 (X=H, Cl, Br) have been measured. The purpose of this study was not specifically to measure lifetime for the first time, but to confirm assignments that had already being made. The results are given in Table VIII. It was not possible to make realistic measurements of the lifetimes of excited states of CH or any of the triatomic fragments except CF_2 $\tilde{A}\,^1B_1$, since they exceed the upper limit which can be measured accurately in this experiment.[31,32] The values measured for the $B\,^2\Delta$ state of CF from CF_2Cl_2 and CF_2Br_2 (18.9 ± 0.2, 17.9 ± 0.2 ns) agree excellently with the long-established phase-shift measurement of 18.8 ns,[52] more recent measurements following electron impact of 20–21 ns,[10–12,53] an *ab initio* calculation,[54] and our measurements on CCl_3F.[1] CF_2H_2 could not be used as the subject molecule as the CF $B-X$ fluorescence was too weak. The value measured for the lifetime of CF $A\,^2\Sigma^+$, 20.0 ± 0.2 ns, from CF_2Cl_2 excited at 19.1 eV is about 30% lower than that determined by a laser-induced fluorescence study of Booth and Hancock,[55] where radiative lifetimes for the $v=0$ and 1 levels were measured to be 26.7 ± 1.8 and 25.6 ± 1.8 ns, respectively. Older measurements yield lifetimes of about 20 ns.[6,52,56] The three values determined for the lifetime of CF_2 $\tilde{A}\,^1B_1$ from CF_2H_2, CF_2Cl_2, and CF_2Br_2 (51.2 ± 0.3, 46.5 ± 0.4, 44.7 ± 0.1 ns) are in good agreement with the results of King, Schenk, and Stephenson.[40] The lifetime measured for the $A\,^2\Delta$ state of CCl from CF_2Cl_2, 21.6 ± 0.6 ns, is much lower than other measurements of the $v=0$ state (~100 ns),[57,58] but is close to the value determined for the $v=1$ state by Larsson, Blomberg, and Siegbahn (17 ns).[58] Thus, there exists the possibility that the fragmentation of CF_2Cl_2 to yield CCl $A\,^2\Delta$ is vibrationally state selective. We should note that the lifetime of CCl $A\,^2\Delta$ measured by us following VUV photoexcitation of CCl_3X (X=F, H, Br) spans the range 39–55 ns.[1] It was suggested then that, as in this work, photodissociation could produce a different distribution of CCl $A\,^2\Delta$ vibrational levels for the three different molecules. The lifetimes determined for the $D'2\,^3\Pi_g$ ion-pair state of Cl_2 and Br_2 (18.6 ± 0.3 and 22.6 ± 0.3 ns) in this work are both consistent with previous studies.[1,11]

V. DISCUSSION

First, we highlight the limitations of the fluorescence experiments. They are only sensitive to excited states of CF_2X_2 that (pre)dissociate to emitting valence states of fragments, and no information is obtained on absolute quantum yields. Likewise, no information is obtained on photodissociation channels that lead to nonfluorescing fragments, or to channels that lead to the ground electronic state of the frag-

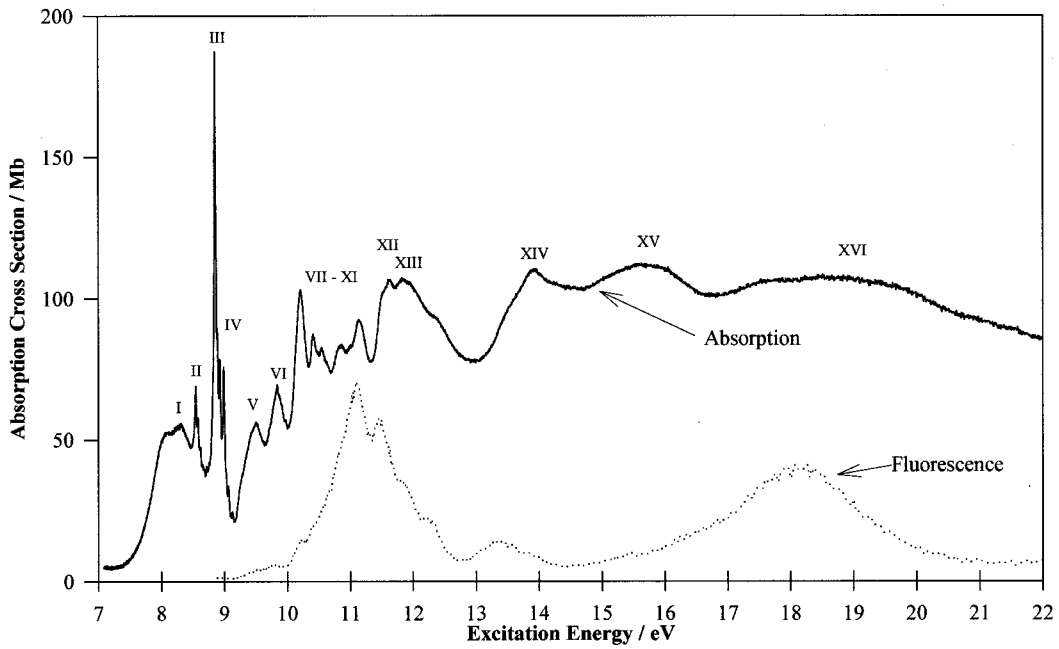

FIG. 10. Vacuum–UV absorption (upper spectrum) and fluorescence excitation (lower spectrum) spectra of CF_2Br_2 recorded at the BESSY1 synchrotron source. The resolution of the spectra are 0.08 and 0.3 nm, respectively. Absorption cross sections are measured in units of Mb (1 Mb$=10^{-18}$ cm^2), fluorescence cross sections in arbitrary units.

ment. Therefore, it should be no surprise that there is often little resemblance between the VUV absorption and fluorescence excitation spectra (Figs. 1, 6, and 10). In particular, these experiments are not sensitive to the simplest photodissociation channel for low-lying Rydberg states of CF_2X_2, which is cleavage of the weakest bond, always C–X, to form the CF_2X free radical. Unlike CF_4 and SiF_4 where photodissociation of such states does lead to fluorescence being observed in the CF_3 and SiF_3 radicals,[17,59] fluorescence from excited states of CF_2X has not been observed. This could arise for one or more of several reasons. First, photodissociation by C–X bond cleavage is a minor channel. Second, photodissociation only produces the ground state of CF_2X. Third, there are no excited states of CF_2X which fluoresce in the range of the UV/visible that our experiment can detect (190–690 nm). This final reason may be the cause of the apparent absence of any emission in CH_2 from CF_2H_2, since the $b\,^1B_1$–$X\,^3B_1$ band of CH_2 is both spin forbidden and occurs predominantly in the near IR.[32] We note that the C–F and C–H bonds have similar strengths in CF_2H_2, the former being only ~0.7 eV stronger than the latter.[31]

The enthalpies for the different dissociation channels that result in the formation of fluorescing fragments are given in Table I. As more than one bond is broken to form each of the observed excited species, there always exists at least two pathways for dissociation. The action spectrum recorded for a particular isolated emission yields the appearance energy (AE) for the formation of the excited fragment. By comparing the AE with the thermodynamic energies given in Table I, it can sometimes be possible to determine the dominant dissociation channel. In our previous study of fluorescence from VUV-excited CCl_3X (X=H, F, Br),[1] this analysis was performed for a large number of fragments. However, the process is made more difficult in this CF_2X_2 study by the fact that the CF_2 $\tilde{A}$–$\tilde{X}$ emission band covers a range of wavelengths, 240–370 nm, where many other emissions occur. Hence, for some fragments it was not possible to record ''true'' action spectra. Second-order radiation from the secondary monochromator also hindered the observation of action spectra for $\lambda_2 > \sim 450$ nm. The discussion, there-

TABLE VI. Assignment of the absorption bands in CF_2Br_2.

Band	Peak position/eV	Assignment	IE/eV[a]	δ
I	8.30	$4b_1$–$5s$	11.56	2.96
II	8.54	$4a_2$–$5s$	12.06	3.03
III	8.85	$4b_2$–$5p$	11.17	2.58
		or $4a_2$–$5s$	12.06	2.94
IV	9.07	$4a_1$–$5s$	12.41	2.98
V	9.50	$4b_2$–$4d$	11.17	1.15
		or $4b_1$–$5p$	11.56	2.43
VI	9.84	$4b_1$–$4d$	11.56	1.19
		or $4a_2$–$5p$	12.06	2.53
		or $3b_2$–$5s$	13.22	2.99
VII	10.21	$4a_1$–$5p$	12.41	2.51
VIII	10.41	$4a_2$–$4d$	12.06	1.13
IX	10.55	$4a_2$–$6s$	12.06	3.00
X	10.86	$4a_1$–$4d$	12.41	1.04
XI	11.14	$3b_2$–$5p$	13.22	2.44
XII	11.63	$3b_2$–$4d$	13.22	1.07
XIII	11.82	$3b_2$–$6s$	13.22	2.88

[a]Vertical ionization energies from Ref. 27.

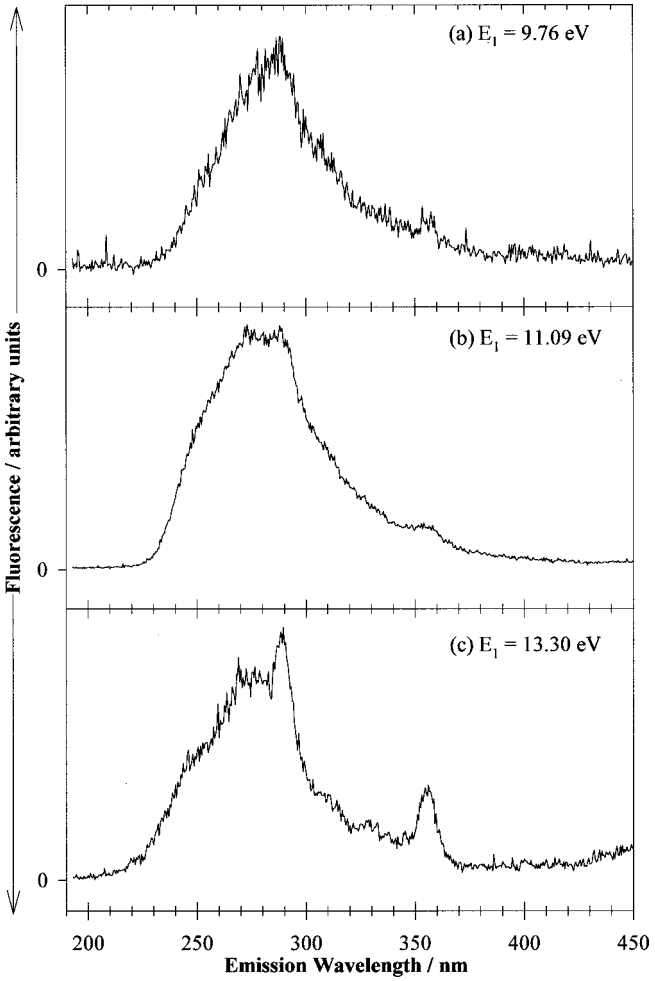

FIG. 11. Dispersed fluorescence spectra recorded at a resolution of 8 nm for CF_2Br_2 photoexcited at (a) 9.76 eV, (b) 11.09 eV, and (c) 13.30 eV.

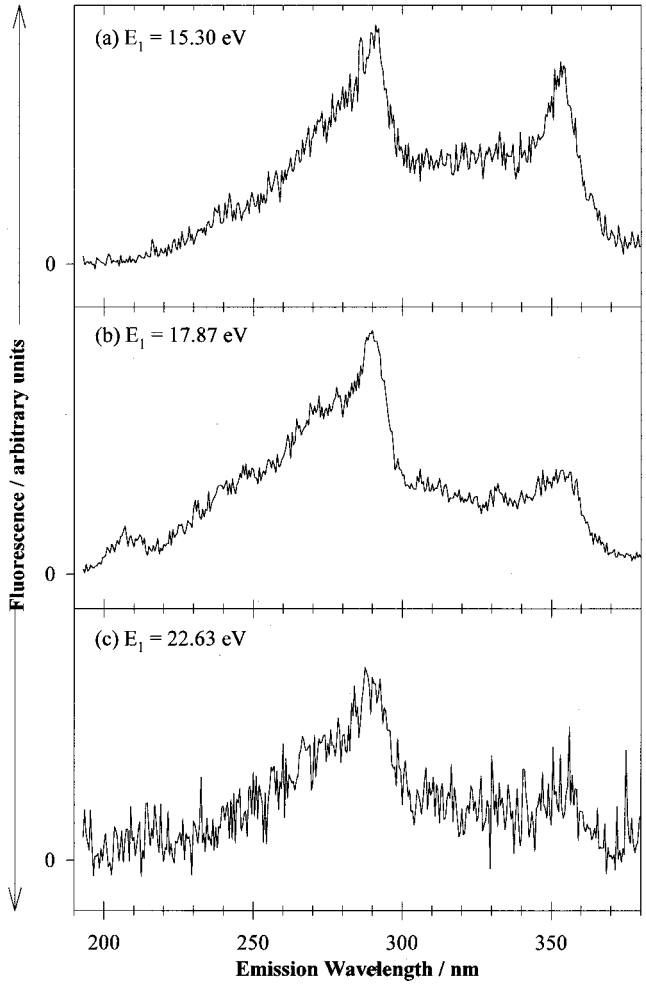

FIG. 12. Dispersed fluorescence spectra recorded at a resolution of 8 nm for CF_2Br_2 photoexcited at (a) 15.30 eV, (b) 17.87 eV, and (c) 22.63 eV.

fore, is limited to the CF_2 $\tilde{A}\,^1B_1$, CF $B\,^2\Delta$, CX (X=H, Cl, Br) $A\,^2\Delta$, Cl_2 and Br_2 $D'2\,^3\Pi_g$, and H* species.

A. CF_2 $\tilde{A}\,^1B_1$

The AEs for forming the CF_2 $\tilde{A}$ state from CF_2H_2, CF_2Cl_2, and CF_2Br_2 are 8.7 ± 0.1, 10.4 ± 0.1, and 9.3 ± 0.2 eV, respectively [Figs. 5(b), 9(b), and 13(b)]. In each case, CF_2 can be formed either with the X_2 molecule or two X atoms, the latter process clearly requiring more energy (Table I). For CF_2H_2, all the emission in bands I and II (Fig. 1) is observed for excitation energies lower than the higher-energy threshold, 11.80 eV, to form two H atoms. Hence, at least for this range of energies, the CF_2 $\tilde{A}$ state must be formed with H_2 and not with two H atoms. For energies greater than 11.8 eV, the fluorescence could be due to the CF_2 $\tilde{A}$ state $+2H$ channel. This situation is totally different from that of CF_2Cl_2 and CF_2Br_2, where the AEs for CF_2 $\tilde{A}$-state production are in close agreement with the energies of the higher dissociation channels, 10.26 and 9.10 eV, respectively. Comparison with the absorption spectra shows that the agreement is not merely coincidental. Hence, for these two molecules it seems likely that dissociation occurs solely by the higher-energy X+X channel. It is not possible to say whether the two C–X bonds break simultaneously or sequentially. It is likely that the anomalous behavior of CF_2H_2 relates to the structure of the transition state. In order for X_2 to be produced, dissociation must proceed via a tightly constrained transition state so that the X–X bond forms while two C–X bonds break. Clearly, such a structure would be sensitive to steric hindrance. Hence, the process is observed for CF_2H_2 where the relatively light H_2 molecule is concerned, but not for CF_2Cl_2 or CF_2Br_2 where bulky Br_2 and Cl_2 molecules must form.

B. CF $B\,^2\Delta$

The AEs for producing CF $B\,^2\Delta$ from CF_2H_2, CF_2Cl_2, and CF_2Br_2 are 12.5 ± 0.3, 18.1 ± 0.2, and 16.0 ± 0.1 eV, respectively [Figs. 5(a), 9(a), and 13(a)]. For CF_2H_2, we note that there is emission at excitation energies below 12.5 eV, but this probably arises from second-order radiation from the primary monochromator. For each molecule there exists three possible dissociation channels whose thermodynamic energies are given in Table I. As with the CF_2 fragment, we observe considerable differences in the behavior of CF_2H_2

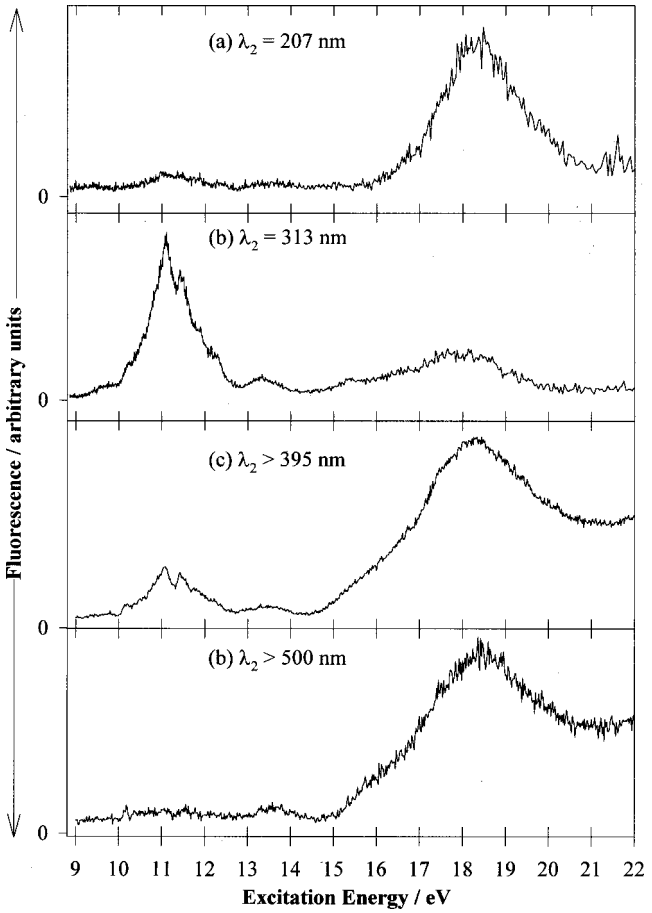

FIG. 13. (a)–(b) Action spectra of CF_2Br_2 recorded at the BESSY1 synchrotron source with a resolution of 0.3 nm for $\lambda_2 = 207$ and 313 nm, respectively. (c)–(d) Fluorescence excitation spectra of CF_2Br_2 recorded at the Daresbury source with a resolution of 0.1 nm. Optical filters ensured that only radiation with (c) $\lambda_2 > 395$ nm and (d) $\lambda_2 > 500$ nm was detected.

compared with CF_2Cl_2 and CF_2Br_2. The experimental thresholds for CF *B*-state production from CF_2Cl_2 and CF_2Br_2 are higher than the thermodynamic energies of all possible dissociation channels. On the basis of thermodynamics alone, therefore, no conclusions regarding the dominant fragmentation pathway can be made. However, since the experimental thresholds are quite close to the thermodynamic energies of the highest-energy channel ($CF_2X_2 \rightarrow CF\ B\,^2\Delta + 2X + F$,) it seems likely that this is the dominant pathway. For CF_2H_2, the experimental threshold is 12.5 ± 0.3 eV, which is extremely close to the thermodynamic energy of the lowest-energy channel ($CF_2H_2 \rightarrow CF\ B\,^2\Delta + HF + H$), 12.74 eV, indicating that, at least for low-excitation energies, dissociation to form these products *must* occur. To form the H–F bond, the dissociation must proceed via a tightly constrained transition state. The situation is then very similar to that concerning the production of $CF_2\ \tilde{A}\,^1B_1$, where steric interaction in the transition state was proposed to account for the anomalous behavior of CF_2H_2 (Sec. V A). In CF_2Cl_2 and CF_2Br_2, where F–Cl and F–Br bonds would have to form, steric hindrance is much greater and presumably prevents dissociation from occurring along this pathway.

TABLE VII. Summary of the emission bands identified following VUV photoexcitation of CF_2Br_2.

Fragment	Appearance energy/eV	E_1 range/eV	λ_2 range/nm	Assignment
$CF_2\ \tilde{A}\,^1B_1$	9.3 ± 0.2	9.3–20.0	240–370	$\tilde{A}\,^1B_1 - \tilde{X}\,^1A_1$
$CFBr\ \tilde{A}\,^1A''$	10.1 ± 0.1	⋯	⋯	$\tilde{A}\,^1A'' - \tilde{X}\,^1A'$
$CBr_2\ \tilde{A}\,^1B_1$	13.2 ± 0.1	⋯	⋯	$\tilde{A}\,^1B_1 - \tilde{X}\,^1A_1$
$Br_2\ D'\,2\,^3\Pi_g$	[a]	⩾13.3	~290	$D'\,2\,^3\Pi_g - A'\,2\,^3\Pi_u$
Br_2*	[a]	⩾13.3	~353	$D'\,2\,^3\Pi_g - {}^3\Delta_u$ [b]
$CF\ B\,^2\Delta$	16.0 ± 0.1	16.0–21.0	207	$B\,^2\Delta - X\,^2\Pi$

[a]Appearance energy between 11.1 and 13.3 eV.
[b]Tentative assignment (Ref. 63).

TABLE VIII. Lifetimes of fragments produced following (pre)dissociation of CF_2H_2, CF_2Cl_2, and CF_2Br_2.

Molecule	E_1/eV	λ_2/nm	Emitter	Lifetime/ns	χ^2
CF_2H_2	13.05	283	$CF_2\ \tilde{A}\,^1B_1$	51.2 ± 03	2.04
CF_2Cl_2	13.05	273	$CF_2\ \tilde{A}\,^1B_1$	46.5 ± 0.4	1.69
	19.07	207	$CF\ B\,^2\Delta$	18.9 ± 0.2	1.06
	19.07	240	$CF\ A\,^2\Sigma^+$	20.0 ± 0.2	1.32
	19.07	278	$CCl\ A\,^2\Delta$	21.6 ± 0.6	4.56
	19.07	256	$Cl_2\ D'\,2\,^3\Pi_g$	18.6 ± 0.3	1.90
CF_2Br_2	11.07	283	$CF_2\ \tilde{A}\,^1B_1$	44.7 ± 0.1	1.49
	13.33	353[a]	Br_2*	22.6 ± 0.3	2.17
	18.23	207	$CF\ B\,^2\Delta$	17.9 ± 0.2	0.99

[a]WG305 filter placed at the exit slit of the secondary monochromator to prevent $CF_2\ \tilde{A}$-state emission being detected.

C. CH $A\,^2\Delta$, CCl $A\,^2\Delta$, CBr $A\,^2\Delta$

The AE for producing CH $A\,^2\Delta$ from CF_2H_2 is 13.8 ± 0.2 eV [Fig. 5(c)]. In Table I, the energies of the three possible dissociation channels are given. For energies below 15.8 eV, dissociation can only proceed via the lowest-energy channel ($CF_2H_2 \rightarrow CH\ A\,^2\Delta + HF + F$). The situation, therefore, is very similar to that involving the formation of CF $B\,^2\Delta$ from CF_2H_2 (Sec. V B). Unfortunately, for reasons given above, an action spectrum could not be measured for the CCl $A\,^2\Delta$ state formed by dissociation of CF_2Cl_2. It is known, however, from the dispersed emission spectra that CCl $A-X$ fluorescence is not observed below 15.5 eV. This information is insufficiently precise to make any comments on the likely dominant dissociation channel involving formation of CCl $A\,^2\Delta$. CBr $A\,^2\Delta - X\,^2\Pi$ fluorescence from CF_2Br_2 is not observed. The fluorescence quantum yield of the upper state, however, is less than unity due to predissociation,[60] thereby reducing the strength of the emission signal.

D. Cl_2 and Br_2 $D'\,2\,^3\Pi_g$

The formation of an excited fluorescing state of Cl_2 and Br_2 is surprising because a Y–Y bond (Y=Cl, Br) must form simultaneously with C–Y bond fission as CF_2Y_2* dissociates. Dissociation must, therefore, proceed via a tightly constrained transition state. Emission from the $D'\,2\,^3\Pi_g$ ion-pair

state of Cl_2 was observed in our CCl_3X (X=F, H, Br) study.[1] Due to the similarity between the threshold energies for Cl_2 $D'2\,^3\Pi_g$ production and the thermodynamic energy of $Cl_2^*+CX+Cl$, it was suggested that this was the preferred dissociation pathway, at least in the range 14–17 eV.[1] It is more difficult to make such clear-cut comments in this CF_2Y_2 study because of the difficulty of obtaining accurate thresholds for Cl_2^* or Br_2^* production from action spectra. For Cl_2^*, however, we can say that the threshold energy is greater than 15.5 eV (Table V), and we note that this is very close to the thermodynamic energy of Cl_2 $D'2\,^3\Pi_g$ +CF+F, 15.56 eV. For Br_2^*, the threshold energy must lie between 11.1 and 13.3 eV (Fig. 11, Table VII), and we note that the thermodynamic energy of Br_2^* $D'2\,^3\Pi_g+CF+F$ is 13.4 eV. It seems likely, therefore, that, as in CCl_3X,[1] Y_2^* forms from $CF_2Y_2^*$ in association with ground-state CF+F, involving the fission of three bonds and the formation of one Y–Y bond. We should note the similarity between the equilibrium bond length of the $D'2\,^3\Pi_g$ ion-pair state of Cl_2, 2.87 A,[33a] and the separation between the two Cl atoms in CF_2Cl_2, 2.87 A.[29] The zero change of bond length, via the Franck–Condon principle, facilitates the production of this excited electronic state of Cl_2. There is also only a very small change in bond length between the Br_2 $D'2\,^3\Pi_g$ ion-pair state (3.17 A) (Ref. 33b) and the Br···Br distance in ground-state CF_2Br_2 (3.21 A).[61]

We comment that while the assignment of the 255 and 290 nm bands to the ion pair to valence transition in Cl_2 and Br_2 $D'2\,^3\Pi_g-A'2\,^3\Pi_u$ is firmly established,[33] there is still no firm assignment of the band in Cl_2 at 305 nm.[62] The lifetime of this band is comparable to that of the $D'2\,^3\Pi_g$ state (~20 ns),[1] suggesting that the upper state of the 305 nm band is indeed the $D'2\,^3\Pi_g$ ion-pair state. The identity of the lower state remains unclear. The 353 nm band in Br_2 has tentatively been assigned to emission from the D' ion-pair state, $D'2\,^3\Pi_g-{}^3\Delta_u$.[63] We note that the lifetime of the upper state of the 353 nm band measured in this work, 22.6 ns (Table VIII), is very similar to that of the $D'2\,^3\Pi_g$ ion-pair state measured from the $D'-A'$ band at 290 nm.[11,64]

E. H* ($n=6,5,4,3$)

The AE for this fragment, 19–21 eV, could only be deduced indirectly by comparing different dispersed fluorescence spectra. It seems likely that the identity of the dominant dissociation channels should not be affected by the Rydberg state ($n=3-6$) in which the H atom is produced. Hence, only the highest-energy $n=6$ state is discussed, and it is assumed that any conclusions drawn also apply to the other states. In the 19–21 eV range, two dissociation channels have thermochemical thresholds, these being $CF_2H_2\rightarrow H^*(n=6)+CF_2+H$ (20.41 eV) and $CF_2H_2\rightarrow H^*(n=6)+HF+CF$ (19.85 eV). In addition, the threshold for $CF_2H_2\rightarrow H^*(n=6)+CF_2H$ lies at 17.71 eV. All other channels involving H* ($n=6$) have thresholds greater than 22 eV (Table I). H* ($n=3-6$) must, therefore, be produced via one or more of these three channels. However, the quality of the data is insufficient to make further comment.

VI. CONCLUSIONS

A comprehensive study of the VUV fluorescence spectroscopy of CF_2X_2 (X=H, Cl, Br) has been presented. The versatility of the synchrotron radiation source has enabled us to employ a wide range of photoexcitation energies, and the ability to disperse the induced fluorescence through a secondary monochromator has made it possible to determine the nature of the emitters. In general, this detail of spectroscopic information is not obtained in nondispersed fluorescence experiments where, using optical filters, only limited information on the range of wavelengths where the emissions occur is determined.[16]

The main practical difficulty with the current experiment was associated with second-order radiation from the secondary monochromator for $\lambda_2>\sim 400$ nm. This problem has since been solved by the use of cut-on filters mounted at the exit slit of this monochromator. Like the CCl_3X(X=F, H, Br) series,[1] all the emission bands are assigned to transitions in neutral fragments formed by (pre)dissociation of the Rydberg states of the parent molecule. No emission from the parent ion is observed. In fragmentations which require the fission of at least two bonds, CF_2Cl_2 and CF_2Br_2 appear to dissociate via the highest-energy fission-only pathways which have low or zero barriers. It is unambiguously shown, however, that CF_2H_2 dissociates to some degree via pathways with tightly constrained transition states and the formation of either a H–H or a H–F bond. This is presumably a steric effect. A detailed analysis of all the dissociation channels was not possible because of the difficulties recording action spectra for all the emitters. There was considerable success, however, in assigning the Rydberg states involved in the primary VUV excitation process, due to the measurement of high-resolution absorption spectra. In hindsight, we conclude that such an approach would have benefited our earlier study on CCl_3X.[1]

ACKNOWLEDGMENTS

The authors thank EPSRC, U.K. for a research grant (GR/M42794) to use the SRS, Daresbury, and the EU Training and Mobility of the Researchers program (Contact No. ERBFMGE-CT-950031) and the British Council (ARC program with Germany, Contract No. 707) for funds to use the BESSY1 source. The authors thank Professor J. Tellinghuisen for helpful suggestions about the electronic spectroscopy of Cl_2 and Br_2, and Dr. W. Zhou (University of Birmingham) for his calculation of the structure of CF_2Br_2 using GAUSSIAN 98. Two of the authors (D.P.S. and R.Y.L.C.) thank EPSRC and the University of Birmingham, respectively, for research studentships.

[1] D. P. Seccombe, R. P. Tuckett, H. Baumgärtel, and H. W. Jochims, Phys. Chem. Chem. Phys. **1**, 773 (1999).
[2] J. J. Tiee, F. B. Wampler, and W. W. Rice, Chem. Phys. Lett. **68**, 403 (1979).
[3] C. L. Sam and J. T. Yardley, Chem. Phys. **61**, 509 (1979).
[4] F. B. Wampler, J. J. Tiee, W. W. Rice, and R. C. Oldenborg, J. Chem. Phys. **71**, 3926 (1979).
[5] Z. J. Jabour and K. Becker, J. Chem. Phys. **90**, 4819 (1989).
[6] H. A. Van Sprang, H. H. Brongersma, and F. J. De Heer, Chem. Phys. **35**, 51 (1978).

[7] G. Allcock and J. W. McConkey, J. Phys. B **11**, 741 (1978).
[8] K. Lieter, P. Scheier, G. Walder, and T. D. Mark, Int. J. Mass Spectrom. Ion Processes **87**, 209 (1989).
[9] O. Keller, C. Mang, M. Nikola, and G. Schulz, Z. Phys. D: At., Mol. Clusters **37**, 315 (1996).
[10] R. Martinez, F. Castano, and M. N. Sanchez Rayo, J. Phys. B **25**, 4951 (1992).
[11] R. Martinez, F. Castano, M. N. Sanchez Rayo, and R. Pereira, Chem. Phys. **172**, 349 (1993).
[12] R. Martinez, I. Merelas, M. N. Sanchez Rayo, and F. Castano, J. Phys. B **28**, 4563 (1995).
[13] T. Ibuki, A. Hiraya, and K. Shobatake, J. Chem. Phys. **90**, 6290 (1989).
[14] C. A. F. Johnson and H. J. Ross, J. Chem. Soc., Faraday Trans. 1 **74**, 2930 (1978).
[15] M. Tsuji, M. Furusana, T. Mizuguchi, T. Muraoka, and Y. Nishimura, J. Chem. Phys. **97**, 245 (1992).
[16] J. C. Creasey, I. R. Lambert, R. P. Tuckett, and A. Hopkirk, Mol. Phys. **71**, 1367 (1990).
[17] H. Biehl, K. J. Boyle, R. P. Tuckett, H. Baumgärtel, and H. W. Jochims, Chem. Phys. **214**, 367 (1997).
[18] C. M. Gregory, M. A. Hayes, G. R. Jones, and E. Pantos, Technical Memorandom, Daresbury Laboratory, Reference No. DL/SCI/TM98E (1994).
[19] A. Hoxha, R. Locht, B. Leyh, D. Dehareng, K. Hottmann, H. W. Jochims, and H. Baumgärtel, Chem. Phys. **260**, 237 (2000).
[20] A. W. Potts, H. J. Lempka, D. G. Streets, and W. C. Price, Philos. Trans. R. Soc. London, Ser. A **268**, 59 (1970).
[21] C. R. Brundle, M. B. Robin, and H. Basch, J. Chem. Phys. **53**, 2196 (1970).
[22] B. P. Pullen, T. A. Carlson, W. E. Moddeman, G. K. Schweitzer, W. E. Bull, and F. A. Grimm, J. Chem. Phys. **53**, 768 (1970).
[23] T. Pradeep and D. A. Shirley, J. Electron Spectrosc. Relat. Phenom. **66**, 125 (1993).
[24] T. Cvitas, H. Gusten, and L. Klansic, J. Chem. Phys. **67**, 2687 (1977).
[25] R. Jadrny, L. Karlsson, L. Mattsson, and K. Siegbahn, Phys. Scr. **16**, 235 (1977).
[26] J. Doucet, R. Gilbert, P. Sauvageau, and C. Sandorfy, J. Chem. Phys. **62**, 366 (1975).
[27] T. Cvitas, H. Gusten, L. Klasinc, I. Novak, and H. Gusten, Int. J. Quantum Chem., Quantum Chem. Symp. **14**, 305 (1980).
[28] I. Novak, J. M. Benson, and A. W. Potts, Chem. Phys. **104**, 153 (1986).
[29] M. W. Chase, J. Phys. Chem. Ref. Data Monogr. **9** (1998).
[30] S. G. Lias, J. E. Bartmess, J. F. Liebman, J. L. Holmes, R. D. Lerin, and W. G. Mallard, J. Phys. Chem. Ref. Data Suppl. **17**, 1 (1988).
[31] K. P. Huber and G. Herzberg, *Molecular Spectra and Molecular Structure* (Van Nostrand, New York, 1979), Vol. IV.
[32] M. E. Jacox, J. Phys. Chem. Ref. Data Monogr. **3** (1994).
[33] (a) J. Tellinghuisen and D. K. Chakraborty, Chem. Phys. Lett. **134**, 565 (1987); (b) A. Sur and J. Tellinghuisen, J. Mol. Spectrosc. **88**, 323 (1981).
[34] P. Wagner and A. B. F. Duncan, J. Am. Chem. Soc. **77**, 2609 (1955).
[35] S. Stokes and A. B. F. Duncan, J. Am. Chem. Soc. **80**, 6177 (1958).
[36] L. Edwards and J. W. Raymonda, J. Am. Chem. Soc. **91**, 5937 (1969).
[37] C. E. Theodosiou, M. Inokuti, and S. T. Manson, At. Data Nucl. Data Tables **35**, 473 (1986).
[38] P. Venkateswarlu, Phys. Rev. **77**, 676 (1950).
[39] R. K. Laird, E. B. Andrews, and R. F. Barrow, Trans. Faraday Soc. **46**, 803 (1950).
[40] D. S. King, P. K. Schenk, and J. C. Stephenson, J. Mol. Spectrosc. **78**, 1 (1979).
[41] A. J. Merer and D. N. Travis, Can. J. Phys. **44**, 1541 (1966).
[42] M. Kakimoto, S. Saito, and E. Hirota, J. Mol. Spectrosc. **88**, 290 (1981).
[43] C. R. Zobel and A. B. F. Duncan, J. Am. Chem. Soc. **77**, 2611 (1955).
[44] J. Doucet, P. Sauvageau, and C. Sandorfy, J. Chem. Phys. **58**, 3708 (1973).
[45] H. W. Jochims, W. Lohr, and H. Baumgärtel, Ber. Bunsenges. Phys. Chem. **80**, 130 (1976).
[46] G. C. King and J. W. McConkey, J. Phys. B **11**, 1861 (1978).
[47] W. Zhang, G. Cooper, T. Ibuki, and C. E. Brion, Chem. Phys. **151**, 357 (1991).
[48] T. X. Xiang, Chem. Phys. Lett. **147**, 183 (1988).
[49] I. Novak, T. Cvitas, and L. Klasinc, J. Chem. Soc., Faraday Trans. 2 **77**, 2049 (1981).
[50] S. K. Zhou, M. S. Zhan, J. L. Shi, and C. X. Whang, Chem. Phys. Lett. **166**, 547 (1990).
[51] J. R. Purdy and B. A. Thrush, Chem. Phys. Lett. **73**, 228 (1980).
[52] J. E. Hesser, J. Chem. Phys. **48**, 2518 (1968).
[53] I. Tokue and Y. Ito, Chem. Phys. **125**, 347 (1988).
[54] A. P. Rendell, C. W. Bauschlicher, and S. R. Langhoff, Chem. Phys. Lett. **163**, 354 (1989).
[55] J. P. Booth and G. Hancock, Chem. Phys. Lett. **150**, 457 (1988).
[56] J. Harrington, A. P. Modica, and D. R. Libby, J. Chem. Phys. **45**, 2720 (1966).
[57] R. A. Gottsho, R. H. Burton, and G. P. Davis, J. Chem. Phys. **77**, 5298 (1982).
[58] M. Larsson, M. R. A. Blomberg, and P. E. M. Siegbahn, Mol. Phys. **46**, 365 (1982).
[59] H. Biehl, K. J. Boyle, D. P. Seccombe, D. M. Smith, R. P. Tuckett, K. R. Yoxall, H. Baumgärtel, and H. W. Jochims, J. Chem. Phys. **108**, 857 (1998).
[60] R. N. Dixon and H. W. Kroto, Trans. Faraday Soc. **59**, 1484 (1963).
[61] W. Zhou, calculation using GAUSSIAN 98 at the MP2/6-311+g(d,p) level (private communication).
[62] J. Tellinghuisen (private communication).
[63] J. Tellinghuisen, P. Berwanger, J. G. Ashmore, and K. S. Wiswanathan, Chem. Phys. Lett. **84**, 528 (1981).
[64] I. Tokue and Y. Ito, Chem. Phys. **125**, 347 (1988).